ERK-mediated phosphorylation of Thr735 in TNFα-converting enzyme and its potential role in TACE protein trafficking

Surinder M. Soond[1,*], Bethany Everson[2], David W. H. Riches[3] and Gillian Murphy[1]

[1]University of Cambridge, Department of Oncology, Cambridge Institute of Medical Research, Hills Road, Cambridge, CB2 2XY, UK
[2]Center for Experimental Therapeutics, University of Pennsylvania School of Medicine, 421 Curie Blvd, Philadelphia, PA 19104, USA
[3]National Jewish Medical and Research Center, Department of Pediatrics, 1400 Jackson Street, Colorado 80206, USA
*Author for correspondence (e-mail: sms45@cam.ac.uk)

Accepted 2 March 2005
Journal of Cell Science 118, 2371-2380 Published by The Company of Biologists 2005
doi:10.1242/jcs.02357

Summary

Tumor necrosis factor α-converting enzyme (TACE/ADAM17) has been implicated in the inducible shedding of numerous cell surface proteins. In light of this, the regulation of TACE catalytic activation and protein maturation has recently received considerable interest in the context of extracellular signal-regulated kinase activation and the subsequent phosphorylation of TACE at residue Thr735. In this study, we analysed the subcellular localisation of TACE derivatives using laser-scanning confocal microscopy and cell surface biotinylation. Whereas WT.TACE- and T735A.TACE-enhanced green fluorescent protein (-eGFP) fusion derivatives of TACE were both found to localise with the endoplasmic reticulum, a phosphomimicking form of TACE (T735E.TACE-eGFP) was found to colocalise predominantly with components of the protein secretory pathway (COPII vesicles and trans-Golgi network). Additionally, upon analysis of biotinylated ectopic TACE, we observed that inducible trafficking of TACE to the cell surface was dependent upon extracellular signal-regulated kinase activation and phosphorylation of Thr735. We conclude from our observations that phosphorylation of TACE at Thr735 highlights a key step in inducible TACE protein trafficking and maturation.

Supplementary material available online at
http://jcs.biologists.org/cgi/content/full/118/11/2371/DC1

Key words: ERK, MAP kinase, TACE phosphorylation, TACE trafficking

Introduction

Members of the ADAMs family of proteins contain a disintegrin and metalloprotease domain and have been shown to exhibit a diverse array of regulatory functions in biological systems, such as the modulation of cell-cell and cell-matrix interactions. Certain members of this family are responsible for the catalytic removal of protein ectodomains and are descriptively termed as 'sheddases' (Black and White, 1998). This has been shown to be the fundamental underlying mechanism for the release of certain cytokines, growth factors and transmembrane receptors (Arribas and Borroto, 2002). The biological activity of ADAMs has also been heavily implicated in Alzheimer's disease, during development and as a key regulator of the inflammatory response (Seals and Courtneidge, 2003).

To date, at least 34 ADAM genes have been described encoding mainly type 1 transmembrane proteins, most of which contain a pro-domain, a metalloprotease domain, a disintegrin and cysteine-rich domain, a transmembrane domain and an intracellular domain (ICD) (Seals and Courtneidge, 2003). Upon the synthesis of ADAMs proteins, the pro-domain inhibits the catalytic activity of the metalloprotease domain, hence its enzymatic removal in a late Golgi compartment that is a critical prerequisite for the maturation of the ADAM protein as it progresses through the secretory pathway (Borroto et al., 2003; Schlondorff et al., 2000). In the case of ADAM17, pro-domain cleavage occurs by pro-protein convertases and furin (Peiretti et al., 2003; Srour et al., 2003).

The ICD of the ADAMs proteins has been shown to be variable in length and sequence. Despite this, the most common motif present in this domain is the PxxP binding site motif for proteins containing an SH-3 domain. This has been extensively characterised for PI-3 kinase and src tyrosine kinase binding in the instances of ADAMs 12 and 15, respectively (Kang et al., 2000; Poghosyan et al., 2002). These observations are functionally consistent with the notion that the ICD may be responsible for mediating 'inside-out' regulation of metalloprotease activity or the 'outside-in' regulation of cell signalling.

TACE/ADAM17 was originally identified by its ability to cleave transmembrane TNF-α to soluble TNF-α in THP-1 cells (Black et al., 1997; Moss et al., 1997). Subsequently, many transmembrane proteins have been identified as substrates for this enzyme, e.g. TNF-Receptor 2 (Reddy et al., 2000), IL-Receptor II (Reddy et al., 2000; Solomon et al., 1999), L-selectin and L1 (Borland et al., 1999), TGF-α (Arribas et al., 1997), erbB4/HER4 (Rio et al., 2000), fractalkine (Garton et al., 2001) and β-amyloid precursor protein (Slack et al., 2001).

Although stimulation with PMA and growth factors has been shown in most cases to enhance the shedding of transmembrane proteins, the underlying mechanisms for this tightly regulated event remain unclear. In the case of ADAM9, PKC-δ has been shown to be directly associated with the ICD and to be required for the shedding of HB-EGF, either after PKC-δ activation or after the phosphorylation of ADAM9 by PKC-δ (Izumi et al., 1998). Similarly, the ICD of TACE has also received considerable attention as a key component in the inducible regulation of TACE activity. To date, the precise role of the ICD in TACE protein maturation and degradation remains unclear. Although the ICD may be dispensable for PMA-induced shedding (Doedens and Black, 2000; Doedens et al., 2003), as yet no evidence has been presented to address whether altered rates of TACE protein maturation and degradation are exhibited by these deletion constructs. As our study was in progress, phosphorylation of pro-TACE at Thr735 and Ser819 was demonstrated upon PMA and growth factor-mediated stimulation of cells. Here, extracellular signal-regulated kinase (ERK) had been shown to interact with TACE and phosphorylate TACE at Thr735 whereas the kinase responsible for the phosphorylation of Ser819 has yet to be identified. Moreover, phosphorylation of Thr735 by ERK was shown to be intrinsically required for the efficient shedding of TrkA by TACE, whereas the precise role of Ser819 phosphorylation on TGF-α shedding still remains to be defined (Diaz-Rodriguez et al., 2002; Fan et al., 2003).

Although ERK modification of TACE ICD has been shown to be critical in efficient inducible shedding of TrkA, the precise physiological significance of this event remains unclear. In this study, we assessed the role of ERK activation and the concurrent modification of TACE at Thr735 by analysing TACE protein maturation and trafficking from the endoplasmic reticulum (ER) to the cell surface. Our observations suggest that the activation of ERK and the consequential modification of TACE at Thr735 is a key step in the physiological regulation of inducible TACE maturation and trafficking to the cell surface.

Materials and Methods

Reagents, antibodies and cells

Phorbol 12-myristate 13-acetate (PMA), U0126 was purchased from Calbiochem (UK). Anti-TACE (C-15), anti-HA probe (Y-11), anti-MEK1 (C-18), anti-phospho threonine (H-2) and anti-ERK2 (D-2) antibodies were purchased from Santa Cruz Biotechnology (USA). Streptavidin-HRP conjugate (21126) was purchased from Pierce (USA) and all secondary antibody-HRP conjugates were purchased from the Jackson Laboratory (USA). Low passage HeLa and COS-7 cells were maintained in complete Dulbecco's Modified Eagle's Medium with 10% v/v fetal bovine serum, 1 mM glutamine, 50 U/ml penicillin and 50 μg/ml streptomycin at 37°C in 5% CO_2. Antibodies for confocal microscopy were used at the following concentration or dilutions: Non-immune goat IgG, anti-calregulin (C-17, 10 μg/ml, Santa Cruz Biotechnology), anti-calregulin (H-170, 10 μg/ml, Santa Cruz Biotechnology) and anti-phospho ERK2 (E-4, 10 μg/ml, Santa Cruz Biotechnology); anti-TGN-46 (1:1000, Serotec) and anti-Sec23 (COPII, 1:500, Affinity Bioreagents).

Plasmids

Full-length wild-type mouse TACE (pWT.TACE) was PCR generated from pMOS/TACE using Vent™ polymerase (New England Biolabs, UK) and cloned into pcDNA3.1+/Zeo (Invitrogen). The DNA sequence of the TACE coding sequence was determined using Big Dye DNA sequencing termination mix (version 2.1, Applied Biosystems). pT735A.TACE and pT735E.TACE mammalian expression plasmids were constructed by PCR using mutated overlapping primers. The resulting cDNA fragments were cloned into pcDNA3.1+/Zeo and their nucleotide sequence verified by sequencing. TACE cDNA fragments were sub-cloned into pEGFP-N1 (BD Clontech), giving plasmids pWT.TACE-eGFP, pT735A.TACE-eGFP and pT735E.TACE-eGFP.

For carboxyl HA epitope tagging of mammalian expression constructs, TACE-derived constructs were cloned into pcDNA3.1+/HA giving the carboxyl HA-tagged TACE constructs pWT.TACE-HA, pT735A.TACE-HA and pT735E.TACE-HA. Mammalian expression plasmids for constitutively active mutated MEK-1 (pMEK-1-HA) and wild-type mouse ERK2 (pWT.ERK2-HA) were PCR cloned using the template plasmid pCAMEK/ERK2-14 (a bi-cistronic plasmid encoding constitutively active *Xenopus* MEK-1 and mouse ERK2). Coding sequences were fused to the HA tag by cloning into pcDNA3.1+/HA. HeLa cells stably expressing WT.TACE were generated by transfecting 10^3 cells using 1 μg of pWT.TACE. 48 hours after transfection the medium was removed and replaced with complete Dulbecco's medium containing 500 μg/ml Zeocin (Invitrogen). Media was replaced every 2 days for 10 days and colonies picked and expanded, before being lysed using NP-40LB and analysed by Western blotting with an anti-TACE ICD antibody (C-15).

Immunoprecipitation

Cells were washed in ice-cold PBS and lysed in 1 ml NP-40LB (50 mM Tris-HCl pH 8.0, 150 mM NaCl, 5 mM EDTA, 1% v/v NP-40, 1 mM phenylmethylsulphonyl fluoride, 20 μg/ml leupeptin, 10 μg/ml aprotinin, 1 mM NaF and 1 mM Na_3VO_4, 10 mM 1,10-phenanthroline, 1 μM BB-94) and the extract cleared by centrifugation at 4°C for 10 minutes at 16,110 ***g***. 5% by volume was removed at this stage for protein analysis by western blotting. Lysates were incubated with 3 μg immunoprecipitating antibody for 3 hours with rotation at 4°C. 50 μl protein A/G-PLUS agarose (Santa Cruz Biotechnology) were added and the reactions incubated overnight at 4°C with rotation. Subsequently, the immune complexes were harvested by centrifugation at 200 ***g*** for 1 minute and then resuspended in NP-40WASH buffer (NP-40LB containing 0.1% v/v NP-40) or NP-40LB for six cycles. Immune complexes were boiled in reducing 1× Laemmli buffer and analysed by western blotting.

Transfection of mammalian cells

Cells were seeded 1 day prior to transfection, at 1.5×10^5 cells per 35 mm dish and at 1×10^4 cells on 13 mm glass coverslips (Agar Scientific, UK). DNA/FuGene 6 complexes were made in serum-free DMEM medium as recommended by the manufacturer (Roche Diagnostics, UK). Transfection mixes were incubated with cells at 37°C for 24 hours.

Radiolabelling total cell proteins

The medium was removed from transfected cells and replaced with phosphate-free DMEM (Invitrogen) containing the above supplements and 2 mCi [^{33}P]orthophosphate for 6 hours (Amersham Pharmacia). Cells were washed twice with ice-cold PBS, lysed in cold NP-40LB and lysates cleared by centrifugation. TACE was immunoprecipitated overnight and immune complexes were washed six times using ice-cold NP-40WASH before being resolved by SDS-PAGE, transferred to nitrocellulose membrane and autoradiographed.

Laser-scanning confocal microscopy

Transfected HeLa cells were fixed in –20°C methanol for 5 minutes then washed three times in PBS. Coverslips were incubated in primary antibody for 1 hour followed by three washes in PBS or as recommended by the manufacturer. Texas Red (1:200, Stratech Scientific, UK) or Alexa 488/546 donkey anti-goat antibody (Molecular Probes, USA) secondary antibodies were used. Coverslips were incubated in secondary antibody for 1 hour before being washed three times in PBS and mounted in Vectashield mounting medium containing DAPI or medium alone (Vectashield Laboratories, UK). Transfected cells were visualised using a Zeiss LSM5 microscope, using 100× objectives. The *z*-stack images were analysed using Zeiss LSM Image browser software and Adobe Photoshop 7 and a selected single *z*-slice is presented in each case.

Pulse-chase analysis of TACE

COS-7 cells were seeded at 2×10^6 cells per 10 cm dish and incubated overnight. The following day cells were transfected using 2 μg pWT.TACE, pT735A.TACE and 6 μg pT735E.TACE using FuGene 6 reagent. 6 hours into the incubation, all cells were treated with 50 μM leupeptin and the incubation continued for 18 hours. The transfected cells were starved for 1 hour in cysteine- and methionine-deficient DMEM medium (containing 50 μM leupeptin) and 210 μCi Redivue ^{35}S PRO-MIX ^{35}S-Cys/^{35}S-Met in vitro cell labelling mix (Amersham Biosciences) was added and the incubation continued for 3 hours at 37°C. The cells were washed twice with ice-cold PBS and then chased in complete DMEM medium (lacking leupeptin) and cell lysates prepared as outlined by (Schlondorff et al., 2000). All lysates were pre-cleared using 50 μl protein A/G-PLUS for 1 hour before TACE was immunoprecipitated by addition of 10 μg of anti-TACE antibody (C-15) for 3 hours before adding 50 μl protein A/G-PLUS agarose beads and the incubation continued overnight at 4°C. Immune complexes were harvested and removed from the agarose beads by heating in 1× Laemmli buffer at 95°C for 5 minutes and all glycoproteins isolated and analysed using concanavalin A sepharose as described (Schlondorff et al., 2000).

Biotinylation of cell surface proteins

Transfected cells were incubated on ice for 5 minutes, washed and cell surface proteins biotinylated with 0.5 mg/ml Sulpho-NHS-LC-biotin [sulphosuccinimidyl-6-(biotinamido)hexanoate] as recommended by the manufacturer (Pierce). Biotinylated cells were lysed in 1.5 ml NP-40LB and TACE-HA derivatives immunoprecipitated overnight before being washed six times in ice-cold NP-40LB and resolved using 10% SDS-PAGE followed by western blotting using streptavidin-HRP conjugated antibodies as recommended by the manufacturer (Pierce). Prior to immunoprecipitation, 50 μl whole cell lysate (WCL) was removed for future protein analysis (by Western blotting) to elucidate positive expression of transiently expressed proteins.

Results

TACE is phosphorylated at Thr735 by ERK in intact COS-7 cells

To dissect a potential role of activated ERK in TACE regulation, we initially asked whether GST-TACE ICD could be inducibly phosphorylated in vitro in an active ERK-dependent manner using supernatants derived from stimulated THP-1 and U937 cells. Our findings suggested that GST-TACE ICD could be phosphorylated upon the stimulation of cells for 10 minutes with PMA, which could be abrogated upon the pretreatment of cells with U0126 and the immunodepletion of ERK from PMA-stimulated cell supernatants (Fig. S1 in supplementary material). Additionally, TNF-α, IL-6, MCP-1 and EGF were also found to activate a component in U937 and THP-1 cells that could mediate the ERK-dependent phosphorylation of GST-TACE ICD in vitro (Fig. S2 in supplementary material). Moreover, we precisely mapped the ERK-directed phosphorylation site in GST-TACE.ICD to Thr735 using commercially available constitutively active ERK2 with C-terminal deletion derivatives of GST-TACE ICD, pGST.694-828(T735A) and pGST.694-828(T735E) as the substrates. Our findings were in good agreement with others (Diaz-Rodriguez et al., 2002), who found that the ERK-mediated phosphorylation site in the TACE ICD mapped to Thr735 (Fig. S3 in supplementary material).

Next we addressed whether TACE can co-compartmentalise and consequently be phosphorylated with activated ERK in intact cells by coexpression of TACE with constitutively active MEK-1 and WT.ERK2 (Robinson and Cobb, 1997). Therefore, we transfected COS-7 cells with pWT.TACE and pWT.ERK2 in the presence or absence of pCA.MEK-1 and incubated the cells with [^{33}P]orthophosphate for 6 hours, as demonstrated for TNF-Receptor 1 phosphorylation (Cottin et al., 1999). When cells were co-transfected with TACE, constitutively active MEK-1 and WT.ERK2, pro-TACE (120 kDa) was maximally phosphorylated in an ERK activation-dependent manner (Fig. 1A, top panel), which is in good agreement with previously published observations (Diaz-Rodriguez et al., 2002). However, in light of the recent observations that TACE may also undergo phosphorylation at Ser819 upon ERK activation (Fan et al., 2003), we next asked whether the ERK-dependent phosphorylation of pro-TACE observed (Fig. 1A) was due to phosphorylation at Thr735. Therefore, we expressed WT.TACE and T735A.TACE in COS-7 cells in the presence of CA.MEK-1 and WT.ERK2, purifying TACE by immunoprecipitation and analysing its phosphorylation status using western blotting with a phosphothreonine-specific antibody (α-pThr). A 120 kDa protein corresponding to pro-WT.TACE was phosphorylated in the presence of active ERK2, which was abolished upon mutation of Thr735 to Ala735 (T735A.TACE) (Fig. 1B, top panel). Interestingly, TACE was detected by western blotting as a very faint doublet band (highlighted by arrows), which is strongly indicative of post-translational modification of proteins by phosphorylation. Collectively, these observations suggest that ectopic pro-TACE (120 kDa) can undergo phosphorylation at Thr735 in an ERK activation-dependent manner in COS-7 cells.

WT.TACE-eGFP resides in the ER

To dissect the functional consequences of ERK-directed phosphorylation of the TACE ICD, we asked whether phosphorylation at Thr735 could modulate the intracellular location of TACE. For this purpose, HeLa cells were utilised to localise WT.TACE-eGFP and T735A.TACE-eGFP as they are morphologically suitable for confocal microscopy. Both TACE derivatives were observed to be significantly colocalised with the intracellular ER marker calregulin (Fig. 2A). This was not an artifact of eGFP fusion, as stably expressed WT.TACE in HeLa cells (WT.HeLa) was also predominantly localised in the ER (Fig. 2B, top panels) and by western blotting was shown to have a molecular mass corresponding to that of pro-TACE

(see Fig. 5B). As a control, negative staining of WT.HeLa cells with non-immune IgG antibodies (data not shown) and untransfected HeLa cells showed that the anti-TACE antibody was specific for the TACE protein (Fig. 2B, bottom panels). Interestingly, we also observed faint nuclear staining of expressed TACE, the function of which is unknown. Additionally, COS-7 cells expressing WT.TACE-eGFP and T735A.TACE-eGFP were analysed by confocal microscopy and the proteins found to strongly colocalise with calregulin (data not shown).

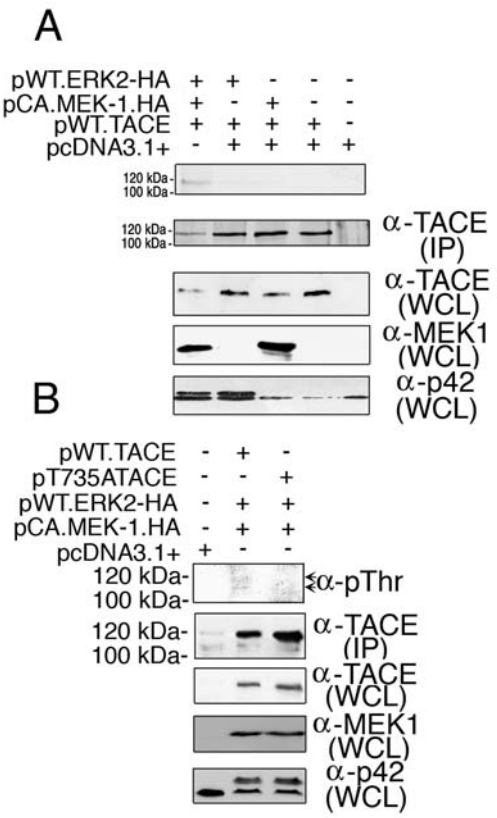

Fig. 1. TACE phosphorylation at Thr735 in intact COS-7 cells is ERK activation-dependent. (A) COS-7 cells were transfected with pcDNA3.1+ (1 μg), pWT.TACE (0.5 μg), pCA.MEK-1.HA (0.25 μg) and/or pWT.ERK-HA (0.25 μg) for 24 hours. Amounts of transfected DNA were kept equivalent to 1 μg using pcDNA3.1+/Zeo. Cells were incubated in the presence of 2 mCi [^{33}P]orthophosphate for 6 hours before the cells were lysed and TACE immunoprecipitated with the anti-TACE ICD antibody. Immune complexes were washed, resolved using SDS-PAGE and western transfer followed by autoradiography (top panel). The same membrane was probed with the anti-TACE ICD antibody to reveal immunoprecipitated TACE protein (α-TACE IP panel). Whole cell lysates (WCL) were also analysed by western blotting to determine the expression levels of TACE, CA.MEK-1.HA and WT.ERK2-HA (lower three panels). (B) Cells were transfected with expression plasmids for WT- and T735A-TACE and TACE protein as in A, and isolated 24 hours later by immunoprecipitation. Immune complexes were washed and probed with an anti-phosphothreonine monoclonal antibody (α-pThr, top panel) and anti-TACE (second panel). WCL were also analysed for expression of TACE, MEK-1 and ERK2 (lower three panels). Arrows highlight the detected TACE species.

Active ERK induces WT.TACE-eGFP relocalisation

Activation of ERK and the subsequent phosphorylation of TNF-Receptor 1 and leukaemia inhibitory factor receptor, alters their subcellular compartmentalisation and is one way the activity of such proteins is tightly regulated upon their exposure to mitogenic stimuli (Blanchard et al., 2000; Cottin et al., 2001). Thus, we asked if ER-resident TACE could be mobilised in an ERK-dependent manner by coexpressing it with constitutively active MEK-1-activated ERK in HeLa cells. Coexpression of CA.MEK-1 or WT.ERK2 with WT.TACE-eGFP and phospho-null T735A.TACE-eGFP did not affect the overall subcellular distribution of the TACE proteins (Fig. 3A). However, coexpression of constitutively active MEK-1 and WT.ERK with WT.TACE-eGFP resulted in the redistribution of WT.TACE-eGFP from the ER to intracellular vesicular structures that are distinct from the ER or are ER-derived. Similarly, upon analysis of T735A.TACE-eGFP, we found that this mutant derivative remained compartmentalised predominantly in the ER (Fig. 3B). Therefore, we concluded that in the presence of active ERK, TACE-eGFP no longer seems to be significantly localised in the ER network and that residue Thr735 is critically important for this change in TACE-eGFP distribution to occur.

T735E.TACE-eGFP resides in cytoplasmic punctate vesicles

To focus on the specific requirement of TACE subcellular localisation on Thr735 phosphorylation, we analysed a phosphomimicking mutant of TACE (T735E.TACE-eGFP) using confocal microscopy. Upon expression of 3 μg pT735E.TACE-eGFP in HeLa cells, a staining pattern consistent with intracellular punctuate staining that was readily distinct from ER staining (as for WT and T735A.TACE) was observed (Fig. 4). Additionally, a similar staining pattern was observed upon the expression of T735E.TACE in HeLa cells, followed by immunostaining with anti-TACE ICD antibodies (data not shown), proving that eGFP was not mislocalising the protein. To address whether this staining pattern was due to T735E.TACE entering the protein transport network, we sought to colocalise this mutant with the ER protein marker calregulin (David et al., 1993), ER-Golgi transport marker Sec-23/COPII (Barlowe et al., 1994) and trans-Golgi network protein TGN-46 (Prescott et al., 1997). T735E.TACE-eGFP colocalised minimally with calregulin and significantly with Sec-23 and TGN-46 (Fig. 4). Collectively, these data suggest that modification of TACE Thr735 may be implicated in the subcellular redistribution of TACE.

TACE Thr735 modification augments pro-TACE protein maturation

As T735E.TACE colocalised with subcellular markers specific for the TGN, we addressed whether proteolytic maturation of pro-T735E.TACE to mature T735E.TACE was comparatively quicker than pro-WT.TACE (Endres et al., 2003; Peiretti et al., 2003). Upon expression of our TACE constructs in COS-7 cells, we observed immunoprecipitated WT.TACE, T735A.TACE (120 kDa) and T735E.TACE (100 kDa), which correspond to the sizes of pro- and mature TACE, respectively

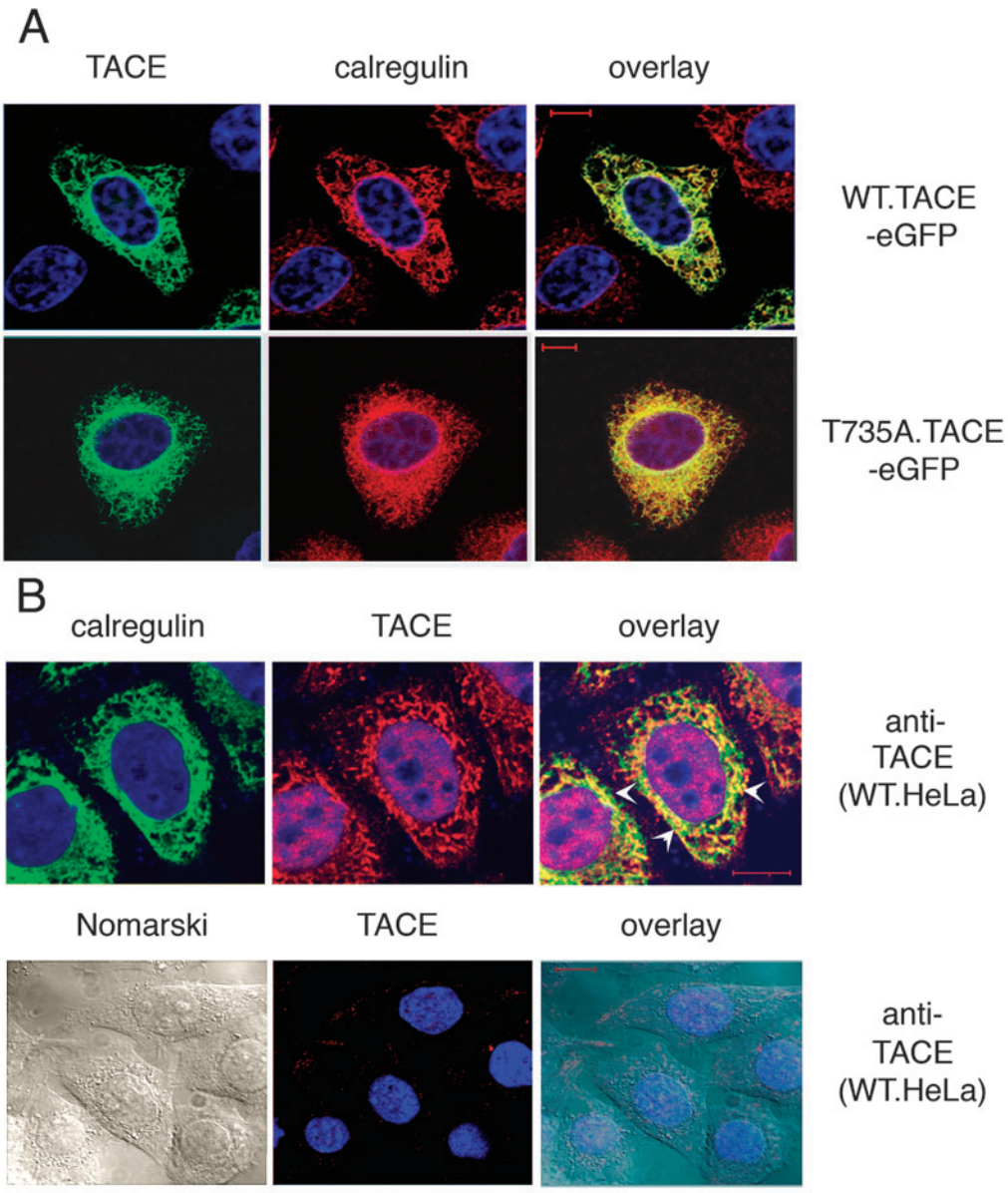

Fig. 2. WT.TACE-eGFP and T735A.TACE-eGFP proteins reside in the ER. (A) HeLa cells were transfected with 0.3 μg pWT.TACE-eGFP and pT735A.TACE-eGFP, fixed using methanol and stained for the ER-specific marker, calregulin (C-17) and Alexa 546 donkey anti-goat secondary antibodies. The coverslips were mounted and visualised using laser-scanning confocal microscopy. The TACE-eGFP protein, ER and nuclei are green, red and blue, respectively. (B) HeLa cells stably expressing WT.TACE (WT.HeLa) were seeded on coverslips and the following day fixed using methanol, stained for TACE using anti-TACE antibody (C-15) and Texas Red-conjugated donkey anti-goat secondary antibodies and the ER stained using anti-calregulin (H-170) and Alexa 488 donkey anti-goat secondary antibodies. Cells were visualised using laser-scanning confocal microscopy with the ER in green, TACE in red, nuclei (stained using DAPI) in blue and colocalisation highlighted with arrowheads (top panels). Untransfected HeLa cells were treated identically and stained using anti-TACE (C-15) primary antibody followed by Alexa 546 donkey anti-goat secondary antibodies. Red and blue channels for TACE and nuclei are shown, respectively (bottom panels). Bar, 10 μm.

(Fig. 5A). These data supported our observations from Figs 2 and 4 that suggested WT.TACE (like T735A.TACE) localised with the ER and that T735E.TACE localised to numerous subcellular compartments, indicating that T735E.TACE is readily processed to mature TACE. Moreover, untagged TACE stably expressed at relatively lower levels in HeLa cells was found to correspond to the molecular mass of pro-TACE (120 kDa, Fig. 5B), which colocalised with the ER marker calregulin (see Fig. 2B). This also implies that transient overexpression of TACE does not have the effect of it artificially residing in the ER.

Although TACE has been demonstrated to undergo phosphorylation at Ser819 in an ERK-dependent manner, we addressed the exclusive role of Thr735 modification on pro-TACE turnover using pulse-chase analysis. Consequently, for T735E.TACE to be visualised as pro-T735E.TACE, we increased the amount of plasmid used in preparation of the transfection mix, in comparison to the amounts used for Fig. 5A. We compared the turnover rates of expressed pro-T735E.TACE with pro-WT.TACE and pro-T735A.TACE (Fig. 5C). Our findings suggested that expressed pro-WT.TACE and pro-T735A.TACE had approximate half-lives that spanned 3-6 and 6-12 hours, respectively. In contrast, expressed pro-T735E.TACE had a significantly shorter half-life that spanned 0-3 hours, after which mature T735E.TACE levels were observed to diminish.

Taken together, these observations suggest that modification of TACE at Thr735 may be responsible for the progression of pro-TACE through the secretory pathway permitting its proteolytic processing to mature TACE, or may be responsible for its degradation.

ERK-dependent phosphorylation of TACE at Thr735 signals translocation of TACE to the cell surface

Following our previous observations, we then addressed whether the cell surface levels of TACE may be regulated by ERK phosphorylation at Thr735. Accordingly, we analysed

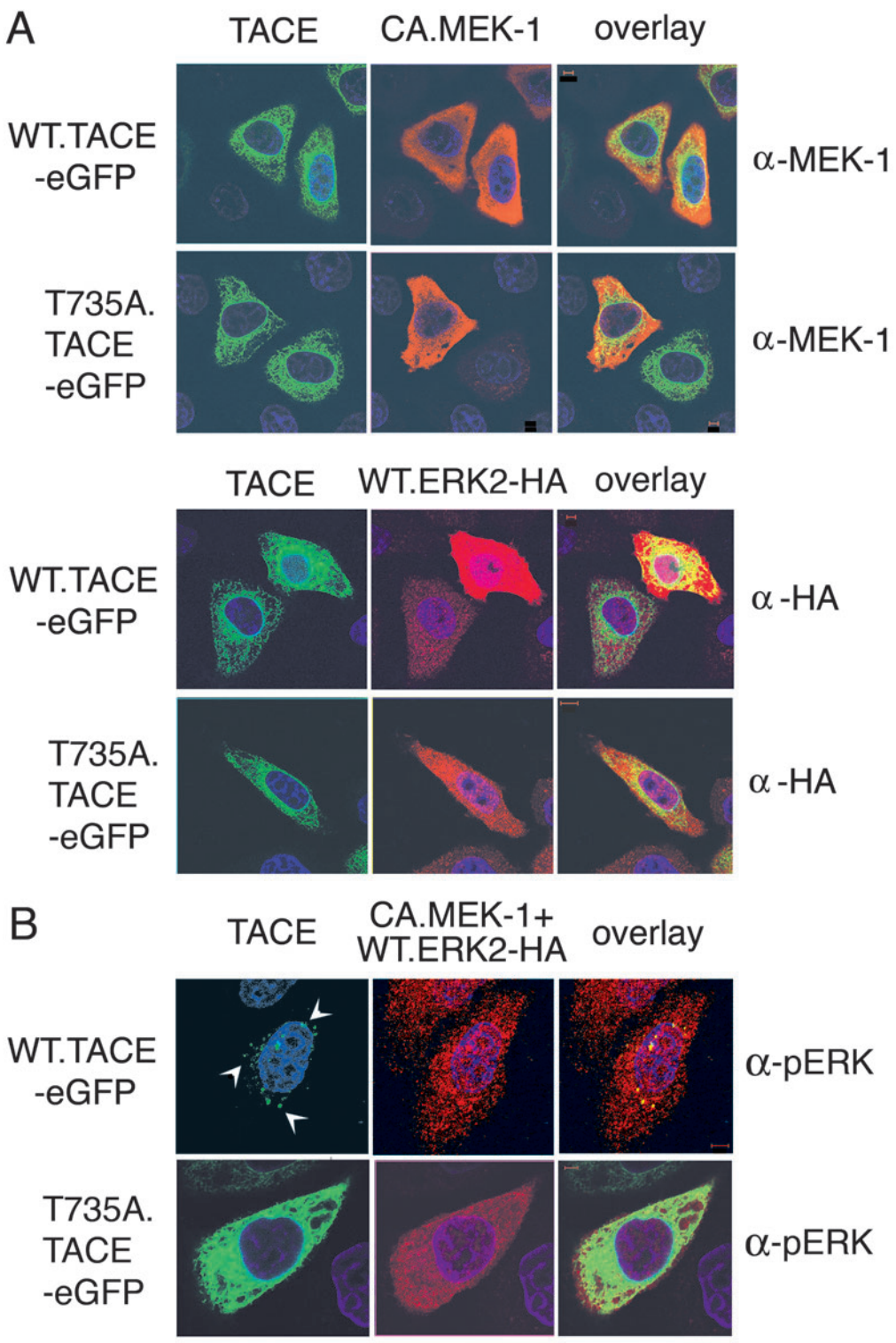

Fig. 3. Subcellular distribution of TACE-eGFP changes with the coexpression of active ERK2. (A) HeLa cells were transfected with either 0.3 μg pWT.TACE-GFP or pT735A.TACE-eGFP, with or without 0.1 μg of pCA.MEK-1.HA and/or pWT.ERK2-HA. DNA amounts were kept equivalent using pcDNA3.1+/Zeo. Cells were fixed in methanol and stained for constitutively active MEK-1 (α-MEK-1), WT.ERK-HA (α-HA), or active phosphor-ERK2 (α-pERK2 in B), before being visualised using laser-scanning confocal microscopy. TACE-eGFP, CA.MEK-1 and/or ERK2 are green and red respectively, whereas the nuclei are blue. The arrowheads highlight a change in the subcellular location of TACE-eGFP protein. Bar, 10 μm.

cell surface HA tagged mature TACE expression upon stimulating TACE-expressing HeLa cells with PMA. Transfected HeLa cells expressing pWT.TACE-HA were stimulated with 1 μM PMA or carrier (DMSO) over a time course of 30 minutes. Cells were surface biotinylated and total TACE immunoprecipitated using an anti-HA antibody and immune complexes analysed by western blotting with streptavidin-HRP. A 100 kDa TACE species (representative of mature TACE) was observed to maximally increase at the cell surface after 10 minutes of stimulation with PMA, after which it declined (Fig. 6A). This result is consistent with the observation that WT.TACE-eGFP localisation is modified when cells are treated with PMA. Upon analysis of the whole cell lysates using western blot analysis with an anti-HA antibody, an intracellular TACE species corresponding to 120 kDa (representative of pro-TACE) was positively detected, which transiently declined in response to stimulating cells with PMA. Interestingly, TACE species corresponding to mature TACE (100 kDa) were readily detected after purification in immune complexes (as highlighted in Fig. 5), probably owing to a relatively low abundance, as only 3% of the total lysates were analysed to determine pro-TACE expression levels.

To address whether the PMA-mediated transient increase in cell surface TACE was due to ERK-dependent phosphorylation of pro-TACE at Thr735, the same experiment was repeated using the expression constructs for WT.TACE-HA and T735A.TACE-HA. Additionally, cells were pre-treated with the MEK-1 inhibitor U0126 (or DMSO) for a period of 30

minutes and each set of cells stimulated with PMA for 5 and 10 minutes prior to the biotinylation of cell surface proteins. After TACE was immunoprecipitated, immune complexes were resolved and western blotted against streptavidin-HRP. A 100 kDa species of cell surface TACE (corresponding to mature TACE) increased in quantity following exposure to PMA for 5 and 10 minutes, which could be abrogated upon the pre-incubation of TACE-expressing cells with U0126 (Fig. 6B). Pro-TACE expression was determined to be positive in these cells by analysis of equal volumes of whole cell lysates by western blotting using an anti-HA antibody. Moreover, partial intracellular depletion of expressed pro-TACE in response to PMA stimulation was observed (as seen in Fig. 6A).

In cells expressing T735A.TACE-HA, no biotinylated TACE species corresponding to mature TACE (100 kDa) were detected after 5 or 10 minutes of stimulation of cells with PMA or 10 minutes with carrier (Fig. 6C). Similarly, cell lysates were analysed for the expression of T735A.TACE-HA using western blotting and were found to express TACE positively as a 120 kDa species that did not show any indication of being intracellularly depleted in response to the PMA treatment of cells. Moreover, HeLa cells expressing pWT.TACE-eGFP or pT735A.TACE-eGFP at 18 hours post-transfection were stimulated with DMSO (30 minutes) or 1 μM PMA and cells were fixed at timed intervals and visualised using immunofluorescence microscopy. Upon stimulation of cells with PMA at 10, 20 and 30 minutes, a punctate staining pattern (readily distinct from the ER staining pattern seen in Fig. 2A) was observed for WT.TACE-eGFP expression and not for T735A.TACE-eGFP expression (Fig. S5 in supplementary material). Collectively, these observations suggest that HeLa cells expressing ectopic TACE exhibit increased amounts of mature TACE at the cell surface in response to PMA stimulation and that this occurs owing to TACE protein trafficking and phosphorylation at Thr735 in an active ERK-dependent manner.

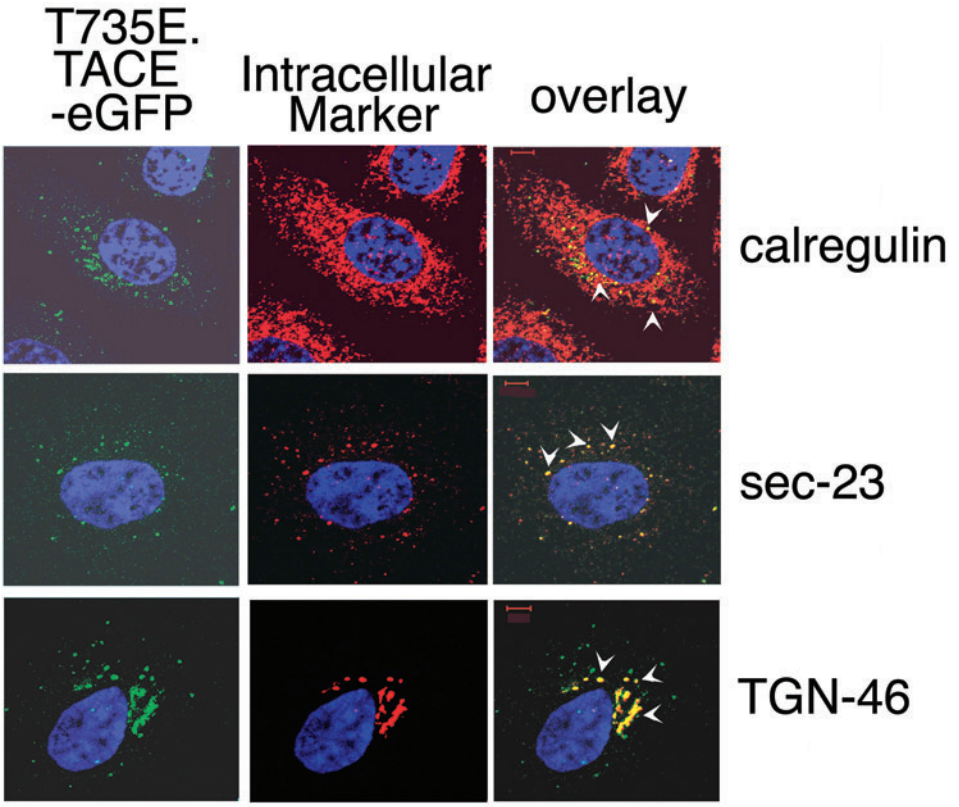

Fig. 4. T735E.TACE-eGFP colocalises with components of the cells protein secretory pathway. HeLa cells were transfected with 3 μg pT735E.TACE-eGFP and incubated at 37°C for 24 hours. Cells were fixed in methanol, followed by immunostaining with antibodies specific for the ER (calregulin), COPII vesicles (Sec-23) and trans-Golgi network (TGN-46) and visualised using laser-scanning confocal microscopy. T735E.TACE-eGFP and the subcellular markers are highlighted in green and red (respectively) whereas the nuclei are shown in blue. Positive colocalisation is highlighted with white arrowheads. Bar, 10 μm.

Discussion

The function of TACE is intrinsic to the regulation of inflammation and sheds a plethora of substrates, from signalling ligands to receptors. Therefore, TACE activity must be tightly regulated for an efficient and effective inflammatory response. Consequently, the inducible nature of TACE activation has received considerable interest, particularly in light of PKC and MAPK-mediated regulation. The fundamental importance of this modification has also been addressed and highlighted in studies where the active ERK-dependent TACE-mediated shedding of TrkA, TGF-α and p75 neurotrophin receptor have been demonstrated (Diaz-Rodriguez et al., 2002; Weskamp et al., 2004).

In this study, we addressed how the exclusive ERK-directed modification of Thr735 in the TACE ICD affects TACE trafficking. Initially, using the pharmacological antagonist U0126 to inhibit ERK activation and immunodepletion of activated ERK (derived from stimulated THP-1 and U937 cells) followed by in vitro kinase of supernatants toward GST fused mutants of the TACE ICD, we confirmed that the TACE ICD is inducibly phosphorylated at Thr735 in vitro and is dependent upon ERK activation. In addition to precisely mapping the ERK phosphorylation site to Thr735 in TACE, we demonstrated that pro-TACE compartmentalises with active ERK and consequently undergoes phosphorylation at Thr735. Moreover, the inducible phosphorylation of pro-TACE at Thr735 was reported in intact HEK-293 cells with which our data is in very strong agreement (Diaz-Rodriguez et al., 2002). These authors found that the optimum inducible shedding of TrkA was dependent upon ERK-mediated phosphorylation at Thr735 of TACE (Diaz-Rodriguez et al., 2002).

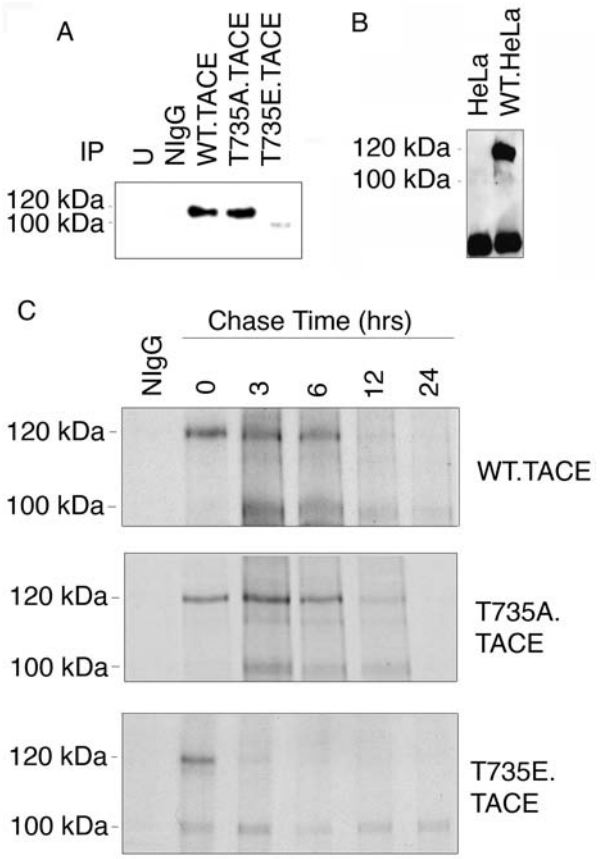

Fig. 5. The molecular mass of T735E.TACE corresponds to mature TACE and is processed to maturity quicker than pro-WT.TACE. (A) COS-7 cells were transfected with 3 μg pcDNA3.1+ (lane U) or 3 μg pWT.TACE (lane NIgG and WT.TACE), pT735A.TACE (lane T735A.TACE) and pT735E.TACE (lane T735E.TACE). Cells transfected with pT735E.TACE were treated with 50 μM leupeptin for 18 hours after 6 hours of transfection. Twenty-four hours after transfection, the cells were lysed and TACE was immunoprecipitated using non-immune IgG antibodies (lane NIgG) or the anti-TACE ICD specific antibody. Immune complexes were washed with NP-40LB, and analysed by western blotting with the anti-TACE ICD antibody (C-15). (B) Similarly, 2×10^6 WT.HeLa or untransfected HeLa cells were seeded overnight and TACE immunoprecipitated using the anti-TACE antibody (C-15). After extensively washing the immune complexes using NP-40LB they were analysed by western blotting using an anti-TACE antibody (C-15). (C) COS-7 cells were transfected with pWT.TACE, pT735A.TACE and pT735E.TACE and treated with 50 μM leupeptin for 18 hours after 6 hours of transfection. Cells were radiolabelled for 3 hours with [^{35}S]methionine/cysteine in the presence of 50 μM leupeptin, washed and chased in complete medium (lacking leupeptin) for the time indicated. TACE was purified and analysed by SDS-PAGE and autoradiography.

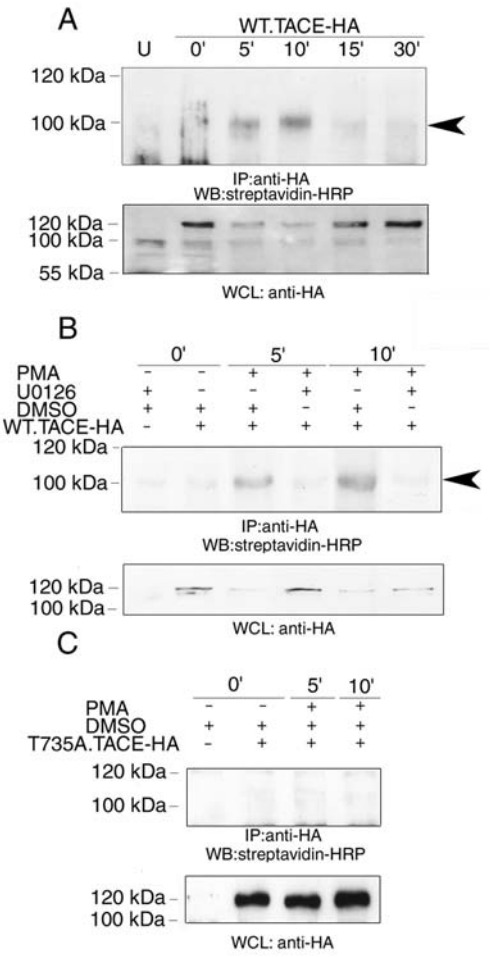

Fig. 6. PMA stimulation of cells causes the translocation of TACE to the cell surface in an ERK phosphorylation-dependent fashion. (A) HeLa cells transfected with 1 μg pcDNA3.1+ (Lane U) or pWT.TACE-HA were pre-incubated with 10 μM U0126 or carrier (DMSO) for 30 minutes, 24 hours after transfection. Cells were stimulated with 1 μM PMA at 37°C for the time points shown (in minutes) before cell surface proteins were biotinylated and TACE immunoprecipitated using anti-HA antibodies (C-15). Immune complexes were washed and analysed by western blotting with streptavidin-HRP (top panel). Equal volumes of whole cell lysates (3% input) were also analysed following biotinylation by western blotting using an anti-HA antibody to detect pro-TACE (lower panel). HeLa cells were transfected with 1 μg pWT.TACE-HA (B) and pT735A.TACE-HA (C) and 24 hours after transfection treated with 10 μM U0126 or carrier (DMSO) at 37°C for 30 minutes. Cells were stimulated at 37°C with 1 μM PMA for the times stated (or carrier for 10 minutes) before cell surface proteins were biotinylated and TACE immunoprecipitated then analysed by western blotting with streptavidin-HRP. Whole cell lysates (3% input) were also analysed by western blotting for the expression of pro-TACE (lower panels in B and C). The arrowheads indicate mature TACE (100 kDa).

Consequently, we pursued the hypothesis that pro-TACE phosphorylation by ERK may be required as a signal for its subcellular translocation from the ER in HeLa cells, permitting its maturation, presumably by furin and pro-protein convertases (Borroto et al., 2003; Endres et al., 2003; Peiretti et al., 2003; Srour et al., 2003). Although the consequences of stimulating cells with PMA on TACE activation has been addressed in this context, the majority of studies have only touched upon the underlying effects on TACE protein trafficking (Diaz-Rodriguez et al., 2002; Endres et al., 2003). Upon the transient expression of WT.TACE, we found it to reside predominantly in the ER, which we hypothesised may serve as an intracellular pool of inactive TACE that can be rapidly mobilised and proteolytically activated upon cell stimulation. These observations are in good agreement with

previously published data where TACE has been shown to reside in the ER (Diaz-Rodriguez et al., 2002; Schlondorff et al., 2000), and further demonstrates that an inability to phosphorylate TACE does not affect its basal localisation. However, previous attempts to show an intracellular redistribution of TACE by immunofluorescence microscopy after stimulating COS-7 expressing TACE cells with PMA for 30 minutes have been inconclusive (Schlondorff et al., 2000). We propose that this may have been due to differences in the amounts of PMA used during stimulation (we used approximately 20 times excess by comparison), as in our hands expressed TACE translocating to the cell surface from an intracellular ER store in HeLa cells occurs transiently and as rapidly as 5-10 minutes after PMA stimulation and also exhibits an intracellular staining pattern distinct to ER staining (Fig. S5 in supplementary material).

Although endogenous TACE has also been detected at the cell surface (Borroto et al., 2003; Doedens and Black, 2000; Schlondorff et al., 2000), the precise mechanisms and the role of ERK mediated TACE phosphorylation in this context maybe more complex than envisaged. Taken together with the observation that purified T735E.TACE can correspond to the molecular mass of mature TACE, we have two hypotheses that are currently being explored in model cell systems: (1) ERK-mediated phosphorylation of pro-TACE may cause it to translocate from the ER to the TGN, followed by translocation to the cell surface; and/or (2) ERK-mediated phosphorylation of cell-surface mature TACE (at Thr735) may signal the internalisation and lysosomal degradation of TACE.

First, in support of the role of Thr735 phosphorylation in mediating TACE translocation from the ER to the cell surface, 120 kDa pro-TACE was the predominant TACE species that underwent phosphorylation by ERK in COS cells. Our observation that T735E.TACE-eGFP co-localises significantly with the markers for ER-Golgi transport (Sec-23) and the TGN marker (TGN-46), coupled with it having the molecular mass of mature TACE, supports the hypothesis that Thr735 phosphorylation may serve to translocate TACE from the ER through the secretory pathway, in HeLa cells. Consequently, T735E.TACE-eGFP may also confer resistance to Endo-H treatment in comparison to ER-resident TACE derivatives (Schlondorff et al., 2000). Additionally, by using pulse-chase analysis we found that T735E.TACE was processed from pro-TACE to mature TACE significantly faster than WT.TACE and T735A.TACE. In our study, WT.TACE matured significantly quicker than endogenous TACE in COS-7 cells possibly because our study analysed expressed TACE (Schlondorff et al., 2000). Additionally, these findings are also consistent with the half-lives of expressed ADAM9 and ADAM15 (Lum et al., 1998; Roghani et al., 1999). Moreover, increased biotinylated cell surface TACE in the presence of PMA stimulation and a partial (but obvious) decrease in intracellular pro-TACE levels further support ERK-mediated anterograde trafficking of TACE. Collectively, these observations are supported by our findings where WT.TACE-eGFP is seen to reside in an intracellular compartment distinct from the ER (or ER derived compartments) upon PMA stimulation of cells using immunofluorescence microscopy (Fig. S5 in supplementary material).

Second, based upon previous observations, a phorbol ester-inducible decrease in the surface pool of functional TACE in the cell has been demonstrated (Doedens and Black, 2000; Endres et al., 2003). In this context, it is also conceivable that phosphorylation of TACE at Thr735 may be involved in routing cell surface TACE for lysosomal degradation. This is supported in part by our observations that T735E.TACE has the same molecular mass as mature TACE (100 kDa), can colocalise significantly with early endosomes and the lysosomal marker LAMP1 (Fig. S4 in supplementary material) and in comparison to WT.TACE and T735A.TACE, has a relatively short half-life and low abundance in cell lysates. Additionally, it has been shown that TACE catalytic activity is a prerequisite for TACE to undergo endocytosis from the cell surface (Doedens and Black, 2000). Consequently, we propose that the 100 kDa T735E derivative of TACE may constitute a catalytically active form of TACE, based upon its molecular mass (Schlondorff et al., 2000), and due to it positively co-localising with the endosomal marker EEA1 (Fig. S4 in supplementary material). However, further work to address these issues is warranted.

Therefore, despite the ICD of TACE being dispensable for inducible TACE shedding, its potential regulatory properties in TACE protein trafficking and activation are becoming increasingly clear. Supported by the fact that the TACE ICD can interact with key signalling components such as protein tyrosine phosphatase 1 (Zheng et al., 2002) and coupled with the fact that TACE ICD can undergo phosphorylation, a novel (and critical) role for the TACE ICD in regulating the catalytic status and the steady-state levels of intracellular TACE is becoming apparent.

In summary, we have assigned a potential role for the ERK-mediated modification of TACE ICD at Thr735. This is based on our observations that expressed pro-TACE becomes phosphorylated by ERK in intact cells and that one of the consequences of this is the inducible translocation of expressed TACE from the ER to the cell surface (which is dependent upon ERK activation), after which it may undergo internalisation and degradation. Collectively, our observations suggest a novel function for the TACE ICD in TACE protein trafficking, which is dependent upon MAPK phosphorylation.

This work was supported by the Wellcome Trust (S.M.S.) and in part from PHS grants HL55549, HL68628 and HL65326 from the National Institutes of Health (D.W.H.R.). We would like to acknowledge Sue J. Atkinson, Christian Roghi and the CIMR Microscopy Unit (Mark Bowen and Matthew J. Gratian) for their assistance and Dalya R. Rosner for proofreading this manuscript.

References

Arribas, J. and Borroto, A. (2002). Protein ectodomain shedding. *Chem. Rev.* **102**, 4627-4638.

Arribas, J., Lâopez-Casillas, F. and Massaguâe, J. (1997). Role of the juxtamembrane domains of the transforming growth factor-alpha precursor and the beta-amyloid precursor protein in regulated ectodomain shedding. *J. Biol. Chem.* **272**, 17160-17165.

Barlowe, C., Orci, L., Yeung, T., Hosobuchi, M., Hamamoto, S., Salama, N., Rexach, M. F., Ravazzola, M., Amherdt, M. and Schekman, R. (1994). COPII: a membrane coat formed by Sec proteins that drive vesicle budding from the endoplasmic reticulum. *Cell* **77**, 895-907.

Black, R. A. and White, J. M. (1998). ADAMs: focus on the protease domain. *Curr. Opin. Cell Biol.* **10**, 654-659.

Black, R. A., Rauch, C. T., Kozlosky, C. J., Peschon, J. J., Slack, J. L., Wolfson, M. F., Castner, B. J., Stocking, K. L., Reddy, P., Srinivasan, S. et al. (1997). A metalloproteinase disintegrin that releases tumour-necrosis factor-alpha from cells. *Nature* **385**, 729-733.

Blanchard, F., Duplomb, L., Wang, Y., Robledo, O., Kinzie, E., Pitard, V., Godard, A., Jacques, Y. and Baumann, H. (2000). Stimulation of

leukemia inhibitory factor receptor degradation by extracellular signal-regulated kinase. *J. Biol. Chem.* **275**, 28793-28801.

Borland, G., Murphy, G. and Ager, A. (1999). Tissue inhibitor of metalloproteinases-3 inhibits shedding of L-selectin from leukocytes. *J. Biol. Chem.* **274**, 2810-2815.

Borroto, A., Ruiz-Paz, S., de la Torre, T. V., Borrell-Pages, M., Merlos-Suarez, A., Pandiella, A., Blobel, C. P., Baselga, J. and Arribas, J. (2003). Impaired trafficking and activation of tumor necrosis factor-alpha-converting enzyme in cell mutants defective in protein ectodomain shedding. *J. Biol. Chem.* **278**, 25933-25939.

Cottin, V., van Linden, A. and Riches, D. W. (1999). Phosphorylation of tumor necrosis factor receptor CD120a (p55) by p42(mapk/erk2) induces changes in its subcellular localization. *J. Biol. Chem.* **274**, 32975-32987.

Cottin, V., van Linden, A. A. and Riches, D. W. (2001). Phosphorylation of the tumor necrosis factor receptor CD120a (p55) recruits Bcl-2 and protects against apoptosis. *J. Biol. Chem.* **276**, 17252-17260.

David, V., Hochstenbach, F., Rajagopalan, S. and Brenner, M. B. (1993). Interaction with newly synthesized and retained proteins in the endoplasmic reticulum suggests a chaperone function for human integral membrane protein IP90 (calnexin). *J. Biol. Chem.* **268**, 9585-9592.

Diaz-Rodriguez, E., Montero, J. C., Esparis-Ogando, A., Yuste, L. and Pandiella, A. (2002). Extracellular signal-regulated kinase phosphorylates tumor necrosis factor alpha-converting enzyme at threonine 735: a potential role in regulated shedding. *Mol. Biol. Cell* **13**, 2031-2044.

Doedens, J. R. and Black, R. A. (2000). Stimulation-induced down-regulation of tumor necrosis factor-alpha converting enzyme. *J. Biol. Chem.* **275**, 14598-14607.

Doedens, J. R., Mahimkar, R. M. and Black, R. A. (2003). TACE/ADAM-17 enzymatic activity is increased in response to cellular stimulation. *Biochem. Biophys. Res. Commun.* **308**, 331-338.

Endres, K., Anders, A., Kojro, E., Gilbert, S., Fahrenholz, F. and Postina, R. (2003). Tumor necrosis factor-alpha converting enzyme is processed by proprotein-convertases to its mature form which is degraded upon phorbol ester stimulation. *Eur. J. Cell Biol. FEBS.* **270**, 2386-2393.

Fan, H., Turck, C. W. and Derynck, R. (2003). Characterization of growth factor-induced serine phosphorylation of tumor necrosis factor-alpha converting enzyme and of an alternatively translated polypeptide. *J. Biol. Chem.* **278**, 18617-18627.

Garton, K. J., Gough, P. J., Blobel, C. P., Murphy, G., Greaves, D. R., Dempsey, P. J. and Raines, E. W. (2001). Tumor necrosis factor-alpha-converting enzyme (ADAM17) mediates the cleavage and shedding of fractalkine (CX3CL1). *J. Biol. Chem.* **276**, 37993-38001.

Izumi, Y., Hirata, M., Hasuwa, H., Iwamoto, R., Umata, T., Miyado, K., Tamai, Y., Kurisaki, T., Sehara-Fujisawa, A., Ohno, S. et al. (1998). A metalloprotease-disintegrin, MDC9/meltrin-gamma/ADAM9 and PKCdelta are involved in TPA-induced ectodomain shedding of membrane-anchored heparin-binding EGF-like growth factor. *EMBO J.* **17**, 7260-7272.

Kang, Q., Cao, Y. and Zolkiewska, A. (2000). Metalloprotease-disintegrin ADAM 12 binds to the SH3 domain of Src and activates Src tyrosine kinase in C2C12 cells. *Biochem. J.* **352**, 883-892.

Lum, L., Reid, M. S. and Blobel, C. P. (1998). Intracellular maturation of the mouse metalloprotease disintegrin MDC15. *J. Biol. Chem.* **273**, 26236-26247.

Moss, M. L., Jin, S. L., Becherer, J. D., Bickett, D. M., Burkhart, W., Chen, W. J., Hassler, D., Leesnitzer, M. T., McGeehan, G., Milla, M. et al. (1997). Structural features and biochemical properties of TNF-alpha converting enzyme (TACE). *J. Neuroimmunol.* **72**, 127-129.

Peiretti, F., Canault, M., Deprez-Beauclair, P., Berthet, V., Bonardo, B., Juhan-Vague, I. and Nalbone, G. (2003). Intracellular maturation and transport of tumor necrosis factor alpha converting enzyme. *Exp. Cell Res.* **285**, 278-285.

Poghosyan, Z., Robbins, S. M., Houslay, M. D., Webster, A., Murphy, G. and Edwards, D. R. (2002). Phosphorylation-dependent interactions between ADAM15 cytoplasmic domain and Src family protein-tyrosine kinases. *J. Biol. Chem.* **277**, 4999-5007.

Prescott, A. R., Lucocq, J. M., James, J., Lister, J. M. and Ponnambalam, S. (1997). Distinct compartmentalization of TGN46 and beta 1,4-galactosyltransferase in HeLa cells. *Eur. J. Cell Biol.* **72**, 238-246.

Reddy, P., Slack, J. L., Davis, R., Cerretti, D. P., Kozlosky, C. J., Blanton, R. A., Shows, D., Peschon, J. J. and Black, R. A. (2000). Functional analysis of the domain structure of tumor necrosis factor-alpha converting enzyme. *J. Biol. Chem.* **275**, 14608-14614.

Rio, C., Buxbaum, J. D., Peschon, J. J. and Corfas, G. (2000). Tumor necrosis factor-alpha-converting enzyme is required for cleavage of erbB4/HER4. *J. Biol. Chem.* **275**, 10379-10387.

Robinson, M. J. and Cobb, M. H. (1997). Mitogen-activated protein kinase pathways. *Curr. Opin. Cell. Biol.* **9**, 180-186.

Roghani, M., Becherer, J. D., Moss, M. L., Atherton, R. E., Erdjument-Bromage, H., Arribas, J., Blackburn, R. K., Weskamp, G., Tempst, P. and Blobel, C. P. (1999). Metalloprotease-disintegrin MDC9: intracellular maturation and catalytic activity. *J. Biol. Chem.* **274**, 3531-3540.

Schlondorff, J., Becherer, J. D. and Blobel, C. P. (2000). Intracellular maturation and localization of the tumour necrosis factor alpha convertase (TACE). *Biochem. J.* **347**, 131-138.

Seals, D. F. and Courtneidge, S. A. (2003). The ADAMs family of metalloproteases: multidomain proteins with multiple functions. *Genes Dev.* **17**, 7-30.

Slack, B. E., Ma, L. K. and Seah, C. C. (2001). Constitutive shedding of the amyloid precursor protein ectodomain is up-regulated by tumour necrosis factor-alpha converting enzyme. *Biochem. J.* **357**, 787-794.

Solomon, K. A., Pesti, N., Wu, G. and Newton, R. C. (1999). Cutting edge: a dominant negative form of TNF-alpha converting enzyme inhibits proTNF and TNFRII secretion. *J. Immunol.* **163**, 4105-4108.

Srour, N., Lebel, A., McMahon, S., Fournier, I., Fugere, M., Day, R. and Dubois, C. M. (2003). TACE/ADAM-17 maturation and activation of sheddase activity require proprotein convertase activity. *FEBS Lett.* **554**, 275-283.

Weskamp, G., Schlondorff, J., Lum, L., Becherer, J. D., Kim, T. W., Saftig, P., Hartmann, D., Murphy, G. and Blobel, C. P. (2004). Evidence for a critical role of the tumor necrosis factor alpha convertase (TACE) in ectodomain shedding of the p75 neurotrophin receptor (p75NTR). *J. Biol. Chem.* **279**, 4241-4249.

Zheng, Y., Schlondorff, J. and Blobel, C. P. (2002). Evidence for regulation of the tumor necrosis factor alpha-convertase (TACE) by protein-tyrosine phosphatase PTPH1. *J. Biol. Chem.* **277**, 42463-42470.